

1       **Phage recombination drives evolution of spore-forming *Bacilli***

2

3       Anna Dragoš<sup>1\*</sup>, Priyadarshini B.<sup>1</sup>, Zahraa Hasan<sup>1</sup>, Mikael Lenz-Strube<sup>2</sup>, Paul J Kempen<sup>3</sup>,  
4       Gergely Maróti<sup>4</sup>, Charlotte Kaspar<sup>5,6</sup>, Baundauna Bose<sup>7</sup>, Briana M. Burton<sup>8</sup>, Ilka B Bischofs<sup>5,6</sup>,  
5       Ákos T. Kovács<sup>1\*</sup>

6       <sup>1</sup> Bacterial Interactions and Evolution Group, Department for Biotechnology and Biomedicine,  
7       Technical University of Denmark, 2800 Kongens Lyngby, Denmark

8       <sup>2</sup> Bacterial Ecophysiology and Biotechnology Group, Department for Biotechnology and  
9       Biomedicine, Technical University of Denmark, 2800 Kongens Lyngby, Denmark

10      <sup>3</sup> Department of Health Technology, Technical University of Denmark, 2800 Kongens Lyngby,  
11      Denmark

12      <sup>4</sup> Institute of Plant Biology, Biological Research Centre, Hungarian Academy of Sciences, H-  
13      6701 Szeged, Hungary

14      <sup>5</sup> BioQuant Center of the University of Heidelberg, 69120 Heidelberg, Germany

15      <sup>6</sup> Max-Planck-Institute for Terrestrial Microbiology, 35043, Marburg, Germany

16      <sup>7</sup> Gro Biosciences, Cambridge, MA 02139

17      <sup>8</sup> Department of Bacteriology, University of Wisconsin, WI 53706, Madison, USA

18

19      \* Corresponding authors: Bacterial Interactions and Evolution Group, Department of  
20      Biotechnology and Biomedicine, Technical University of Denmark, Søtofts Plads Building  
21      221, 2800 Kongens Lyngby, Denmark

22      Tel: +45 26272642; Fax: +45 45 932809; E-mail: [adragos@dtu.dk](mailto:adragos@dtu.dk);

23      Tel: +45 45 252527; Fax: +45 45 932809; E-mail: [atkovacs@dtu.dk](mailto:atkovacs@dtu.dk);

24

25 **Abstract**

26 Phages are the main source of within-species bacterial diversity and drivers of horizontal gene  
27 transfer. Prophage cargo can determine ecological interactions of a bacterium with other  
28 community members, and even its pathogenic potential, but we know little about the  
29 mechanisms that drive genetic diversity of these mobile genetic elements (MGEs). Recently,  
30 we showed that a sporulation selection regime promotes evolutionary changes within SP $\beta$   
31 prophage of *Bacillus subtilis*, leading to direct antagonistic interactions within the population.  
32 Interestingly, SP $\beta$  belongs to the so-called phage regulatory switches that precisely excise from  
33 the chromosome of sporulating mother cells, a phenomenon observed for phages infecting  
34 diverse spore-forming species. Herein, we reveal that under a sporulation selection regime, SP $\beta$   
35 recombines with low copy number phi3Ts phage DNA present within the *B. subtilis* population.  
36 Recombination results in a new prophage occupying a different integration site, as well as the  
37 spontaneous release of virulent phage hybrids. Analysis of *Bacillus* sp. strains suggests that  
38 SP $\beta$  and phi3T belong to a distinct cluster of unusually large phages inserted into sporulation-  
39 related genes that are equipped with a spore-related genetic arsenal. Comparison of *Bacillus*  
40 sp. genomes at global and local ecological scales indicates that these SP $\beta$ -like phages diversify  
41 rapidly, especially in the absence of other MGEs constraining their lytic cycle. Our study  
42 captures inter-phage recombination under an experimentally imposed selection regime, and  
43 reveals the ubiquity of similar phenomena in *Bacillus* sp. genomic data. Therefore, our work is  
44 a stepping stone toward empirical studies on phage evolution, and understanding the eco-  
45 evolutionary relationships between bacteria and their phages.

46

47

48

## 49 **Introduction**

50 Bacteriophages are major regulators of bacteria. Each day, approximately half of all bacterial  
51 biomass is killed by lytic phages, imposing a constant predator-prey evolutionary arms race<sup>1–</sup>  
52 <sup>3</sup>. Moreover, phages reside in 40–50% of bacterial genomes as prophage elements<sup>4</sup>, serving as  
53 a main source of intra-species genetic diversity and gene transfer agents<sup>5</sup>. Although prophages  
54 can be considered genetic parasites, they can also benefit their host with new metabolic  
55 functions, survival strategies or weapons for inter-bacterial warfare<sup>4–6</sup>. Despite the abundance  
56 and relevance of prophages in bacterial genomes, we still understand very little about their  
57 ecological and evolutionary imprint. This knowledge gap is particularly paramount for non-  
58 pathogenic bacterial agents, such as widely applied biocontrol and probiotic bacterial strains  
59 of agricultural and medical importance. Notably, genomes of certain beneficial bacterial genera  
60 (e.g. *Bacillus* sp.) are extremely rich in prophages<sup>7</sup>. Moreover, prophage cargo divergence in  
61 certain *Bacillus* species (e.g. *Bacillus subtilis*) leads to social ‘incompatibility’, which  
62 manifests in strong competitive interactions and physical barriers between bacterial swarms<sup>8,9</sup>.  
63 Currently, we do not understand what promotes diversity within the prophage cargo of closely  
64 related strains.

65         Based on striking mosaicism of prophage genomes, we believe that they  
66 predominantly evolve through recombination<sup>10–12</sup>. Through exchange of functional groups of  
67 genes (modules), phages can rapidly gain or lose functions<sup>11,13</sup>. Recombination between  
68 phages or between phages and their hosts can be either homologous<sup>14,15</sup> or non-homologous<sup>16</sup>,  
69 relying on phage- or host-encoded recombinases<sup>14,17</sup>. It was proposed that gene shuffling  
70 regularly occurs between (functional or defective) prophages and phages that co-infect the  
71 same host bacterium<sup>14</sup>. It was also shown that prophages of naturally competent bacteria (e.g.

72 *B. subtilis*) can recombine with foreign phage DNA via transformation<sup>18</sup>. Finally, phages can  
73 randomly or specifically incorporate fragments of host chromosomes via generalised<sup>19,20</sup> or  
74 specialised<sup>21,22</sup> transduction, respectively, thereby contributing to the spread of antibiotic  
75 resistance<sup>20</sup> or virulence genes<sup>23</sup>. Although evidence from comparative phage genomics  
76 indicates frequent recombination into new phage variants (so-called gene shuffling)<sup>13,24,25</sup>, this  
77 is not reflected in experimental research. Phage recombination has been experimentally studied  
78 using limited models, predominantly *Salmonella typhimurium* P22 with *Escherichia coli*  
79 lambdoid phages<sup>26,27</sup>. Therefore, despite our knowledge of pronounced genomic mosaicism,  
80 empirical research on prophage evolution is relatively limited. Combining such research with  
81 broader comparisons of available host genomes may prove key to understanding the ecology  
82 and evolution of bacteria and phages, including whether prophages serve as a major source of  
83 bacterial within-species diversity, or as regulators.

84           Interestingly, certain prophages of *Bacilli* undergo genetic rearrangements upon  
85 host development, acting as so-called phage regulatory switches (RSs)<sup>28</sup>. RS phages can switch  
86 between integrated and extrachromosomal forms to modulate reproduction and survival of their  
87 hosts, through processes that differ from classical lysogeny or lysis<sup>28</sup>. To date, most  
88 documented RS phages have been detected in Firmicutes as regulators of the sporulation  
89 process<sup>29–32</sup>, associated with vegetative cells transforming into partially dehydrated dormant  
90 spores, and related to resistance to extreme conditions, including starvation for millions of  
91 years<sup>33,34</sup>. Certain *B. subtilis* biocontrol strains carry an SP $\beta$  prophage or its derivative that  
92 integrates into the polysaccharide-related gene *spsM*, and this genetic interruption prevents  
93 robust submerged biofilm formation in the host<sup>29,35</sup>. In addition, in SP $\beta$  prophage-harboring  
94 strains, immediately prior to sporulation the prophage undergoes precise excision and  
95 circularisation, allowing *spsM* reconstitution and expression in the sporulating mother cell. The  
96 resulting *spsM*-related polysaccharide eventually becomes part of the spore coat, contributing

97 to spore dispersability<sup>29</sup>. Besides SP $\beta$ , another prophage-like element named *skin* also  
98 undergoes excision in the mother cell, allowing reconstitution of *sigK* encoding a late  
99 sporulation sigma factor that is necessary for completing the sporulation process<sup>32,36,37</sup>. Similar  
100 mother cell-specific excisions have been observed in other *Bacillus* sp.<sup>29</sup> and in *Clostridium*  
101 sp.<sup>31,38</sup>, but we do not understand what drives such a distinctive relationship between spore-  
102 forming hosts and their phages, nor what eco-evolutionary consequences this has. Interestingly,  
103 SP $\beta$  and *skin* both encompass genes relevant for sporulation, including *sspC* that is crucial for  
104 spore DNA protection and repair<sup>39,40</sup>, and the *rapE*–*phrE* signalling system involved in  
105 sporulation initiation<sup>41,42</sup>. Furthermore, certain prophages can improve or even restore  
106 sporulation in *B. subtilis*<sup>43</sup>, suggesting the possibility of a cooperative relationship between  
107 certain phages and spore-formers.

108 We recently demonstrated that under a repeated imposed sporulation selection  
109 regime, SP $\beta$  prophages of *B. subtilis* undergo major genetic rearrangements, giving rise to new  
110 hybrid phages<sup>44</sup>. Normally, the lytic cycle of SP $\beta$  prophages is blocked by the ICEBs1  
111 (Integrative and Conjugative Element of *B. subtilis*) conjugative element<sup>45</sup>, and new phage  
112 variants are released spontaneously, killing or infecting the original host<sup>44</sup>. Therefore, it is  
113 important to reveal the genetic changes that lead to prophage awakening, and determine  
114 whether similar prophage evolution pathways occur outside the laboratory.

115 Herein, we investigated the triggering cause of diversification and spontaneous  
116 release of SP $\beta$  prophages, and sought evidence for similar diversification of SP $\beta$  taking place  
117 in nature. Using experimental evolution, *de novo* genome sequencing and testing, we showed  
118 that barely detectable, low copy number phage DNA residing in certain *B. subtilis* strains can  
119 propagate under an appropriate selection regime, and hybridise with indigenous prophages.  
120 These new prophage elements modulate host development, most likely through regulatory  
121 genes. Bioinformatic comparison of prophage elements within available *Bacillus* sp. genomes

122 demonstrated that similar recombination may frequently occur in nature between SP $\beta$  and  
123 related phages. Our work shows how diversification of prophages through recombination can  
124 drive early diversification of bacterial populations.

125

## 126 **RESULTS**

### 127 **Strains evolved under a sporulation selection regime carry hybrid prophages**

128 We previously showed that several passages of *B. subtilis* through the dormant spore stage  
129 leads to genome rearrangements within prophage elements and release of phage particles into  
130 the culture medium (Fig. 1A). Some of these phages resemble indigenous SP $\beta$ <sup>46</sup>, but unlike  
131 SP $\beta$  prophages they are produced spontaneously and facilitate killing of the original SP $\beta$   
132 lysogenic strain<sup>44</sup> (Fig. 1B). To further characterise the genetic changes within the prophage  
133 regions of these evolved strains, three isolates (B310mA, B410mB and B410wtB)<sup>44</sup> were  
134 subjected to long-read genome sequencing using the PacBio platform (see Materials and  
135 Methods). *De novo* sequencing revealed the presence of an exogenous SP $\beta$ -like prophage (58%  
136 sequence identity), which was nearly identical to *Bacillus subtilis* phage phi3T (KY030782.1;  
137 99.98% sequence identity)<sup>47</sup> in all three strains (Fig. 1C, Suppl. Fig. 1A). We named these  
138 extrachromosomal phage elements phi3Ts. The only difference between previously sequenced  
139 phi3T and phi3Ts was a 725 bp fragment (labelled 's' for sporulation-derived) within phi3Ts,  
140 replacing the 1265 bp fragment of phi3T (nucleotides 101,429–102,694; Fig. 1D). Strikingly,  
141 the 's' fragment shares no homology with phi3T or *B. subtilis* 168 chromosomes, but it could  
142 be found within SP $\beta$ -like prophages of six *B. subtilis* strains isolated in different regions around  
143 the world (see Materials and Methods; Fig. 1D). In the evolved strains, the phi3Ts prophage  
144 either disrupted the *kamA* gene located ~11 kb from SP $\beta$ , or it created a hybrid with SP $\beta$  with  
145 a ~11 kb fragment deleted between *kamA* and SP $\beta$  (Fig. 1C, Suppl. Fig 1A). In addition,

146 sequencing coverage within the described prophage regions was increased several-fold,  
147 suggesting augmented replication of hybrid phage DNA (Suppl. Fig. 1B, Suppl. dataset 1).

148

### 149 **Hybrid lysogens produce virulent hybrid phages**

150 In view of the presence of phi3Ts, SP $\beta$  and phage hybrids on the chromosomes of the evolved  
151 strains (Fig. 1C, Suppl. Fig 1A), we were curious which phages are spontaneously released into  
152 the medium<sup>44</sup>. Therefore, phages released by the evolved strains were purified from single  
153 plaques and subjected to genome sequencing (see Materials and Methods). Notably, each  
154 evolved strain produced a mix of turbid and clear plaques, but at different relative frequencies  
155 (Suppl. Fig. 1C). Turbid plaques are typical for temperate phages (like SP $\beta$  or phi3T), while  
156 clear plaques are usually formed by phage variants that have lost their ability to enter the  
157 lysogenic cycle<sup>48</sup>. Phage sequencing revealed that the spontaneously produced phages were  
158 either phi3Ts or phi3Ts-SP $\beta$  hybrids (Fig. 1C, Suppl. Fig. 1A, Suppl. Fig. 2). Sequences of all  
159 phages obtained from the turbid plaques matched prophage sequences within the evolved  
160 strains (Fig. 1C, Suppl. Fig. 1A, Suppl. Fig. 2). In addition, the genome of Hyb1<sup>phi3Ts-SP $\beta$</sup>   
161 (released by B310mA) was extended by a ~1.2 kb fragment of the host chromosome (*yozE*,  
162 *yokU*, and part of the *kamA* gene), indicating specialised transduction, a process that occurs  
163 when a phage picks up a fragment of host chromosomal DNA in the immediate vicinity of its  
164 attachment site (Fig. 1C, Suppl. Fig. 2). In contrast to the turbid plaque-creating phages, all  
165 phages obtained from clear plaques were phi3Ts-SP $\beta$  hybrids, which were not present on the  
166 chromosomes of their corresponding producers (Fig. 1C, Suppl. Fig. 1A, Suppl. Fig. 2). This  
167 suggests that phi3Ts-SP $\beta$  recombination not only gave rise to hybrid prophages, but also to a  
168 range of virulent phages. In addition to chromosomal DNA, in strains B410mB and B410wtB  
169 we identified a variety of extrachromosomal phage DNA (epDNA) fragments ranging from

170 10.9 to 66 kb (Fig. 2, Suppl. dataset 1). The epDNA was dominated by phi3Ts-SP $\beta$   
171 recombinants, in which DNA from the two parental phages was joined at the homologous  
172 region (Fig. 2). None of the hybrid epDNA was identical to sequences of hybrid phages  
173 released by the corresponding strains (B410mB and B410wtB; Fig. 2, Suppl. Fig. 2). Finally,  
174 we also noticed that some epDNA fragments contained parts of the bacterial chromosome  
175 adjacent to the phi3Ts integration site, again pointing towards specialised transduction (Fig. 2).

176

### 177 **A sporulation selection regime promotes foreign phage invasion**

178 Next, we aimed to identify the source of phi3Ts DNA in the evolved host genomes, and to  
179 determine whether this DNA was already present in the ancestor *B. subtilis* 168 stock or  
180 acquired as contamination during the evolution experiment. First, we repeated the mapping of  
181 raw sequencing reads from the *B. subtilis* 168 ancestral genome onto selected unique phi3T  
182 regions lacking homology with SP $\beta$ . Indeed, phi3Ts DNA was present in the ancestor strain at  
183 a very low but detectable level, rather than as an extrachromosomal form (Fig. 3, Suppl. Fig.  
184 3A), hence that only subset of cells contained the plasmid-like form of phi3Ts. On the other  
185 hand, phi3T could be clearly detected by mapping of resequencing reads of the evolved strains  
186 (Suppl. Fig. 3A).

187 The presence of phi3Ts DNA fragments in the ancestor was additionally  
188 confirmed by PCR using a series of primer sets specific for unique phi3Ts fragments, phi3Ts-  
189 *kamA* attachment sites, and the *kamA* gene (Suppl. Fig. 4). PCR performed on genomic DNA  
190 of *B. subtilis* 168 resulted in a strong band from the intact *kamA* gene, a weak band from  
191 selected fragments of phi3Ts, and very faint bands indicating *kamA* integration (Suppl. Fig.  
192 4A). Conversely, PCR on genomic DNA extracted from evolved strains showed the presence  
193 of very strong bands for both phi3Ts fragments, and left and right integration sides (except for



194 B310mA in which the right part of *kamA* was absent. As expected, strains B310mA and  
195 B410wtB1 were negative for intact *kamA*, while B410mB gave a weak product, which could  
196 be explained by incorporation of *kamA* into its epDNA (Fig. 2, Suppl. Fig. 4A).

197           The above analysis indicates that low copy number phi3Ts was present in the *B.*  
198 *subtilis* 168 stock from the start. Since *B. subtilis* 168 has been shared among research labs  
199 around the world, low copy number phi3Ts could also be ‘hiding’ in culture stocks of other  
200 research labs. Accidental detection of such low copy number phage DNA is nearly impossible,  
201 because (i) re-sequencing reads matching phi3Ts would be filtered out during standard  
202 mapping pipelines, and (ii) phi3Ts appears to only multiply and manifest itself under specific  
203 selection regimes. To check for possible contamination of other *B. subtilis* stocks with phi3Ts,  
204 we mapped raw re-sequencing data available in the NCBI database to the phi3T genome  
205 (KY030782.1). Analysis of five *B. subtilis* 168 genomes from different laboratories showed  
206 no evidence of phi3Ts contamination, since re-sequencing reads matched fragments with high  
207 homology to phi3T-*B. subtilis* 168 (Suppl. Fig 3B).

208           In addition to resequencing data analysis, we also PCR-screened a larger  
209 collection of *B. subtilis* 168 stocks from different labs around the world<sup>49</sup> for the presence of  
210 phi3Ts. Although the vast majority of tested strains lacked phi3Ts sequences (in agreement  
211 with sequencing data analysis), a very strong band was observed for *B. subtilis* 168  
212 ‘Newcastle’, suggesting that this strain was infected with phi3Ts, or a very similar prophage  
213 (Suppl. Fig. 4B). Further PCR analysis confirmed phage integration into the *kamA* gene, but  
214 also the presence of an intact *kamA*, indicating that a subpopulation of cells could be  
215 pseudolysogenic (Suppl. Fig. 4B). We also confirmed that, similar to the experimentally  
216 evolved strains, the Newcastle 168 strain contained the ‘s’ fragment, a unique sequence  
217 allowing the phi3Ts phage to be distinguished from the previously sequenced phi3T, hence it  
218 is a specific marker for the ‘laboratory’ phage variant (Fig. 1D).

219 As phi3Ts multiplies under a prolonged sporulation selection regime, we  
220 contacted colleagues who also performed experimental evolution with *B. subtilis* strains  
221 imposing the same or similar selection<sup>50,51</sup>. First, we approached a group from the University  
222 of Wisconsin-Madison, with whom we had not previously shared strains, because they  
223 published a study on the evolution of *B. subtilis* strain PY79 (NC\_022898.1) under a prolonged  
224 sporulation selection regime<sup>50</sup>. They kindly agreed to share raw sequencing data obtained from  
225 12 evolved single isolates, and we investigated potential changes within prophage regions, and  
226 searched for the presence of phi3Ts DNA. We did not find any mutations within prophage  
227 regions (Suppl. dataset 2). Furthermore, mapping of raw sequencing reads of evolved PY79  
228 strains to the phi3T genome excluded the presence of phi3T-specific DNA fragments (see  
229 Materials and Methods; Suppl. Fig. 5).

230 We also approached a group from the University of Groningen, who performed  
231 experimental evolution of *B. subtilis* 168 under nutrient-limited conditions in which bacteria  
232 could neither grow nor complete sporulation (due to *sigF* deletion)<sup>51</sup>. Mapping their raw  
233 sequencing reads to the phi3T genome clearly revealed the presence of phi3T-specific reads  
234 (Suppl. Fig. 3C). Similar to our case (Fig. 3, Suppl. Fig. 3A), the phage DNA was already  
235 present at the start, and it either gradually decreased or increased in two different biological  
236 samples (Suppl. Fig. 3C).

237 The above results strongly suggest that the prophage activation scenario requires  
238 not only a sporulation selection regime, but also contamination with low copy number phi3Ts  
239 DNA or phage particles. The exchange of strains between Newcastle University (the origin of  
240 *B. subtilis* 168 PCR-positive for the phi3Ts-specific fragment) and the University of  
241 Groningen, and later between the University of Groningen and our lab, represents a possible  
242 transmission route for phi3Ts.

243 Finally, the evolution experiment performed previously<sup>44</sup> was repeated under the  
244 sporulation selection regime using the undomesticated *B. subtilis* NCIB 3610 (hereafter 3610)  
245 strain in which the presence of phi3Ts DNA could not be detected during analysis of genome  
246 resequencing (Suppl. Fig. 3D, Suppl. Fig. 6A) or by PCR (Suppl. Fig. 6B). This time, alongside  
247 classical heat treatment (20 min at 80°C), a chemical spore-selection method (see Materials  
248 and Methods) was also employed, along with consecutive testing of lytic activity in the culture  
249 supernatant and analysis of the presence of phi3Ts DNA and the integrity of the *kamA* gene at  
250 every transfer (Suppl. Fig. 7). To our surprise, lytic activity (Suppl. Fig. 7A) and the release of  
251 phages (Suppl. Fig. 7B) were observed as early as the fourth transfer when the sporulation  
252 selection regime was applied. Similarly, targeted PCR analysis of host DNA revealed a gradual  
253 increase in the phi3T-specific PCR product and a gradual decrease in the PCR product  
254 corresponding to intact *kamA* (Suppl. Fig. 8). No lytic activity was observed in a parallel  
255 control treatment without the sporulation selection regime (Suppl. Fig. 7A).

256

### 257 **Foreign phages modulate sporulation dynamics**

258 We next explored whether propagation of low copy number phi3Ts DNA and its integration  
259 into the *kamA* gene has any positive fitness effects on *B. subtilis*. Since expression of *kamA* is  
260 dramatically increased upon sporulation entry (*SubtiWiki* website ([http://subtiwiki.uni-](http://subtiwiki.uni-goettingen.de)  
261 [goettingen.de](http://subtiwiki.uni-goettingen.de)), we hypothesised that *kamA* may encode a product that is metabolically costly  
262 and/or toxic for the bacterium, hence the phi3Ts/phi3Ts-SP $\beta$  hybrid lysogen may benefit from  
263 inactivation of this gene (Suppl. Figure 9A). However, competition assays between wild-type  
264 vs.  $\Delta$ *kamA* strains with and without sporulation selection revealed no difference in performance  
265 between strains (Suppl. Fig. 9B).

266 We hypothesised that certain genes encoded by phi3Ts may provide benefits to  
267 the host under a sporulation/spore revival selection regime. Therefore, we examined the  
268 sporulation and spore revival dynamics of *B. subtilis* 3610 deliberately infected with phi3T, a  
269 phage stock isolated from the lysogen available from the Bacillus genetic stock center (BGSC).  
270 We observed that the phi3T lysogen sporulated prematurely compared with the wild-type strain  
271 (Fig. 4). We also observed a general trend indicative of better revival of the phi3T lysogen  
272 (Suppl. Fig. 10A), which may include contributions from faster germination (Suppl. Fig. 10B)  
273 and/or an altered frequency of premature germination during dormancy (Suppl. Fig. 10C).

274 These observations indicate the possibility that phi3T/phi3Ts may encode  
275 proteins that influence the *B. subtilis* life cycle during sporulation and spore revival. Notably,  
276 sporulation regulators have been previously linked to mobile genetic elements (MGEs) in this  
277 species<sup>52-54</sup>. Annotation of phi3Ts and phi3Ts-SP $\beta$  hybrids (see Materials and Methods)  
278 revealed the presence of several genes that could modulate sporulation or spore traits.  
279 Specifically, we found a gene (labelled as *rapX*) encoding a putative Rap phosphatase (Suppl.  
280 Fig. 11, Suppl. Table 1) sharing high amino acid sequence identity with RapA (unique for  
281 phi3Ts) that is known to modulate sporulation timing<sup>55</sup>. We also found that the 's' phi3Ts  
282 marker sequence may encode stationary phase survival protein YuiC (100% confidence Phyre  
283 prediction = 100% confidence), hence we labelled this sequence *spsX* (Suppl. Fig. 11). In  
284 addition, we identified *sspC* that controls spore resistance traits and encodes an acid-soluble  
285 protein involved in spore DNA protection (present on both SP $\beta$  and phi3Ts)<sup>56</sup>. Notably, we did  
286 not find genes that are known to affect spore revival (i.e. germination or spore outgrowth),  
287 suggesting that the effects on spore revival may be conferred indirectly (e.g. by modulation of  
288 sporulation timing)<sup>57</sup>. Together, these results suggest that the spread of phi3Ts under a  
289 prolonged sporulation selection regime might be partly driven by host benefits from the  
290 regulatory arsenal associated with phi3Ts and its hybrids.

291

292 **Recombination between SP $\beta$ -like prophages takes place on global and local ecological**  
293 **scales**

294 To understand the ecological relevance of extensive phage recombination observed under a  
295 sporulation selection regime, we performed global analysis of prophage elements within the *B.*  
296 *subtilis* clade including *B. cereus* for comparison of more distant species (see Materials and  
297 Methods). In a total of 350 fully-assembled genomes, 1365 prophage elements were identified  
298 using Phaster software (Suppl. dataset 3). Interestingly, we could immediately identify a cluster  
299 of rather large (<100 b) prophages integrated close to the replication terminus, just like phi3Ts,  
300 SP $\beta$  or phi3Ts-SP $\beta$  hybrids. These large prophages were found mainly (86%) within  
301 representatives of *B. subtilis*, *B. amyloliquefaciens*, *B. licheniformis* and *B. velezensis* species  
302 (Fig. 5A, Suppl. dataset 3). In total, we selected 78 strains carrying a large prophage close to  
303 the replication terminus for further analysis (see Materials and Methods; Suppl. Fig. 12A).

304           Among these strains we identified 23 (including SP $\beta$  lysogens *B. subtilis* NCBI  
305 3610 and *B. subtilis* 168) in which large prophages had split the *spsM* gene in a manner identical  
306 to SP $\beta$  (Suppl. dataset 3), and four *B. subtilis* isolates in which the *kamA* gene was split by a  
307 prophage region at exactly the same site, as observed in the hybrid lysogens (Suppl. dataset 3).  
308 In the remaining Bacillus strains, the large prophages were mostly integrated close to  
309 sporulation-related genes, including a homolog of *fisB* encoding a sporulation-specific  
310 membrane fission protein (*B. velezensis* SCDB 291), a homolog of *ymaG* encoding an inner-  
311 spore coat protein (*B. atrophaeus* BA59) and a homolog of *cotD* encoding an inner-spore coat  
312 protein (*Bacillus amyloliquefaciens* H). Interestingly, 10 strains carried extrachromosomal  
313 phage DNA (as predicted by Phaster; Suppl. dataset 3), and in one of them (*B. subtilis*  
314 SRCM103612) this epDNA was a truncated version of an SP $\beta$ -like prophage present within

315 the chromosome (Fig. 5B). The SRCM103612 prophage contained regions sharing homology  
316 to both SP $\beta$  and phi3Ts, indicating recombination and an unstable lysogenic cycle within SP $\beta$ -  
317 like recombinant phages in natural *B. subtilis* isolates (Fig. 5B).

318 To assess the within-species conservation of large prophages, we performed  
319 multiple sequence alignment of all the aforementioned prophage sequences. Prophages  
320 clustered according to host species, possibly as a result of phage-host specificity and/or  
321 prophage-host coevolution (Suppl. Fig. 12B). To assess the natural diversity of large SP $\beta$ -like  
322 prophages, we collected *Bacillus* sp. genomes carrying a large prophage splitting *spsM* or *kamA*  
323 (see Materials and Methods) and compared the phylogenetic tree obtained for these strains (see  
324 Materials and Methods) with the phylogenetic tree obtained for their SP $\beta$ -like prophages (Fig.  
325 6AB). The strains could be divided into six phylogenetic clades (Fig. 6A), while prophages  
326 clustered into three clades ('conservative', 'hybrid' and 'diverse'. The 'conservative' clade  
327 comprised prophages that were nearly identical to SP $\beta$ , that were also found within closely  
328 related *B. subtilis* strains (all were members of the 3610 clade; Fig. 6AB). The 'hybrid' clade  
329 comprised phi3T, phi3Ts and all phi3Ts-SP $\beta$  hybrids that evolved in the above described  
330 experiments under a sporulation selection regime (Fig. 6B). Within the 'diverse' clade the  
331 prophage relatedness did not match the phylogenetic relatedness of the host strains (Fig. 6AB).  
332 For example, in phylogenetically distinct NCD-2 and WR11, isolated from different sources  
333 (Suppl. dataset 3), an identical prophage disrupted the *spsM* gene. By contrast, prophages of  
334 closely related strains MB8\_B1 and MB8\_B10 that were isolated from the same mushroom  
335 differed in genetic architecture and in integration site. Indeed, we found that among *B. subtilis*  
336 isolates from the same soil sample below the mushroom<sup>58</sup>, one strain (MB8\_B7) carried an  
337 *spsM*-integrated SP $\beta$  prophage, one strain (MB8\_B1) carried a SP $\beta$ -like prophage in *spsM*, and  
338 one strain (MB8\_B10) carried an SP $\beta$ -like prophage in *kamA* (Fig. 6AB). Additionally, we  
339 noticed that nearly all members of the 'conservative' clade carried an intact copy of iCEBs1

340 that was shown to block the SP $\beta$  lytic cycle<sup>45</sup>, while this element is missing in all members of  
341 the ‘diverse’ clade (Fig. 6B). Finally, we could clearly see modules sharing high homology  
342 with SP $\beta$  and phi3T in the large prophages (Fig. 6C). These results are consistent with our lab  
343 data showing that SP $\beta$ -like phages diversify in nature, and this diversification may be  
344 constrained by other MGEs present on the host chromosome.

345

## 346 **Discussion**

347 The importance of phages in the ecology and evolution of bacteria is indisputable. Interactions  
348 between bacteria and temperate phages are especially complex, because the latter can serve as  
349 both beneficial genetic cargo and as a constant threat of cell death. Genome comparison  
350 suggests that prophage elements undergo pervasive domestication within their hosts that  
351 gradually lose the ability to reproduce via the lytic cycle<sup>59</sup>. Our current work demonstrates an  
352 opposite scenario, where after a prolonged sporulation/spore revival selection regime, a latent  
353 prophage of *B. subtilis* (SP $\beta$ )<sup>44,45</sup> regains its lytic reproductive cycle via recombination with  
354 ‘foreign’ phage DNA (phi3Ts). The fact that phi3Ts only manifests itself under specific  
355 conditions (a prolonged sporulation/spore revival selection regime) is reminiscent of  
356 previously described examples of *Proteobacteria* phages<sup>60,61</sup>. Specifically, the lytic phage SW1  
357 can thrive undetected within *E. coli* populations, but manifests itself in spontaneous plaque  
358 formation after overexpression of a putative methylase from an indigenous cryptic prophage<sup>60</sup>.  
359 Likewise, lytic variants of P22 spontaneously form upon purine starvation of the *Salmonella*  
360 *typhimurium* host<sup>61</sup>. In our case, an increase in phi3Ts DNA copy number and its integration  
361 into the chromosome took place upon application of a sporulation selection regime.

362 Exactly how sporulation promotes the spread of ‘foreign’ phage and its hybrid  
363 derivatives requires further molecular studies. There are two, not mutually exclusive,



364 hypotheses: (a) induction of the phage lytic cycle in a small fraction of sporulating cells leads  
365 to rapid amplification of phi3Ts DNA, infection of other sporulating cells, segregation of phage  
366 DNA into forespores, and trapping of many of its copies in spores, followed by the release of  
367 phages upon germination, as observed previously for lytic *B. subtilis* phages<sup>62,63</sup>; (b) since  
368 phi3T lysogeny (KY030782.1; 99.98% sequence identity with phi3Ts)<sup>47</sup> results in earlier  
369 sporulation and potentially improved spore quality, integration of this phage into the  
370 chromosome may be adaptive for the host. As the functions of most phi3Ts genes are obscure,  
371 it is difficult to identify the potential phage-encoded regulatory genes that could affect the host  
372 life cycle. One possibility is *rap-phr* cassettes (matching *rap* present in phi3T and phi3Ts) that  
373 have been previously found within other MGEs of *B. subtilis*, and have been shown to modulate  
374 the timing of sporulation<sup>52-54</sup>. Phi3Ts phage genes (e.g. *sspC*) could modulate the production  
375 of resistant and viable spores<sup>56</sup> and/or reduce sporulation failure and premature germination<sup>64</sup>.  
376 In addition, the spore revival traits of lysogens may also be indirectly affected by the  
377 modulation of sporulation timing<sup>57</sup>. Whatever the exact molecular mechanism and its  
378 evolutionary driver, the activation of latent prophage elements upon sporulation/spore revival  
379 treatment expands the intriguing connections between sporulation of *Firmicutes* and phages  
380 infecting these species<sup>29,31,43,65-67</sup>.

381           Based on comparison of the sizes and integration sites of prophage elements  
382 within *Bacillus* sp., SPβ and phi3T clearly belong to a distinct prophage group. These phages  
383 appear extremely large (2–3-fold larger than average prophages), and they possess  
384 sophisticated communication systems that are potentially capable of sensing the frequency of  
385 infected hosts<sup>47,68</sup> or biosynthetic gene clusters<sup>69,70</sup>, and functional genes related to host  
386 dormancy<sup>71,72</sup>. All these features, combined with regulatory excision upon sporulation, indicate  
387 strong codependence between SPβ-like phages and their hosts. A high level of homology  
388 between SPβ and phi3Ts offers extensive regions for homologous recombination, which can



389 be additionally promoted by the recombination machinery involved in natural competence<sup>73</sup>  
390 and in non-homologous end-joining repair<sup>74</sup>. It appears that the absence of other mobile genetic  
391 elements (e.g. ICEBs1) constraining the phage lytic cycle<sup>45</sup> may also correlate with a higher  
392 level of phage diversification. However, whether sporulation promotes recombination between  
393 SP $\beta$  and phi3Ts alongside phi3Ts amplification remains to be investigated. It is possible that  
394 such phage recombination could be facilitated by regulatory excision of SP $\beta$  from the  
395 chromosome in the sporulating mother cell<sup>29,30</sup>. It also remains to be confirmed whether all  
396 *spsM*-splitting prophage elements, such as SP $\beta$ , behave like regulatory switches as previously  
397 suggested<sup>29</sup>. The disruption of *kamA* by phi3Ts, SP $\beta$ -phi3Ts hybrids, and SP $\beta$ -like prophages  
398 in *Bacilli* suggests that this gene might also be controlled by regulatory excision.  
399 Recombination between SP $\beta$  and phi3Ts under a sporulation/spore revival selection regime is  
400 an example how new regulatory phage-host relationships may evolve.

401 In addition to regulatory switch behaviour, *Bacilli* and their large SP $\beta$ -like  
402 prophages pervasively recombine during sporulation, providing new model systems to study  
403 bacterial evolution in which phages serve as an evolutionary driving force. Ecological  
404 relevance of prophage recombination observed under lab conditions is well supported by  
405 natural diversity within the same group of prophage elements on global and local ecological  
406 scales. The crucial role of prophage elements on ecological interactions within closely related  
407 strains has already been demonstrated for other species<sup>8,60,75,76</sup>. Herein, we showed that such  
408 antagonism emerges during the early steps of phage diversification, which may suggest that  
409 speciation of prophage elements may be the first step toward speciation of host bacteria.  
410 Finally, our work sheds new light on the interplay between bacteria and their phages; while  
411 temperate phages commonly undergo domestication<sup>59</sup>, they may easily regain genetic mobility  
412 by recombination with other phages, thereby altering the physiology, social interactions and  
413 evolution of their host.

414

415

## 416 **Materials and Methods**

417 **Strains and cultivation conditions.** Supplementary Table S2 describes the bacterial strains  
418 used in this study and Supplementary Table S3 lists all phages used in this work. Plasmids and  
419 oligonucleotides used for cloning purposes to construct some of the strains used here are listed  
420 in Supplementary Table S4. Strains were routinely maintained in lysogeny broth (LB) medium  
421 (LB-Lennox, Carl Roth; 10 g/l tryptone, 5 g/l yeast extract, and 5 g/l NaCl).

422 Strain DTUB200 was obtained by infecting DK1042 (WT NCBI 3610) with a phage phi3T  
423 obtained from CU1065. DTUB201 ( $\Delta$ SP $\beta$ ) was obtained by transforming DK1042 with gDNA  
424 obtained from SPmini and selecting for erythromycin-resistant colonies. Strain DTUB202  
425 ( $\Delta$ kamA) was obtained by transforming DK1042 with gDNA obtained from BKK19690 and  
426 selecting for kanamycin-resistant colonies. All modifications of DK1042 were verified by PCR  
427 followed by Sanger sequencing. Strain DTUB203 ( $P_L$ -gfp) was obtained by transforming  
428 DK1042 with pDTUB206 ( $P_L$ -gfp) plasmid and selecting for chloramphenicol-resistant  
429 colonies. To obtain this plasmid,  $P_L$  promoter was amplified from *B. subtilis* 168 gDNA using  
430 oAD10 and oAD11, introducing the EcoRI and NheI restriction sites. The PCR product was  
431 then ligated into pre-digested pGFP-rrnB plasmid to obtain pDTUB206. Strains DTUB204 ( $P_L$ -  
432 *gfp*<sup>phi3T</sup>) and DTUB205 ( $P_L$ -*gfp*<sup>phi3Ts</sup>) were obtain by infecting the DTUB203 with phi3T and  
433 phi3Ts phages, respectively.

434

## 435 **Genome sequencing and analysis**

436 Phage sequencing was performed by Illumina MiSeq instrument and a 2x250 nt paired-end  
437 chemistry (MiSeq Reagent Kit v2 (500-cycles). Primary data analysis (base-calling) was

438 carried out with Bbcl2fastq<sup>^</sup> software (v2.17.1.14, Illumina). In vitro fragment libraries were  
439 prepared using the NEBNext<sup>®</sup> Ultra<sup>™</sup> II DNA Library Prep Kit for Illumina. Reads were  
440 quality and length trimmed in CLC Genomics Workbench Tool 11.0 and *de novo* genome  
441 assembly was performed using SPAdes-3.13.0-Linux and CLC Genomics Workbench 11.0.

442 *De novo* sequencing and assembly of B310mA, B410mB and B410wtB genomes was  
443 performed by Functional Genomics Center Zurich, from genomic DNA of exponentially grown  
444 cultures, extracted using the EURex Bacterial and Yeast Genomic DNA Kit. Resequencing of  
445 168 ancestor (ancestor of B310mA, B410mB and B410wtB) was described in our previous  
446 manuscript<sup>44</sup>.

447 Evolved PY79 strains (presented in Suppl. dataset 2) were obtained as previously described<sup>50</sup>.  
448 Samples for whole-genome sequencing were prepared according to the Illumina Multiplexing  
449 Sample Preparation Guide, using NEBNext reagents and Illumina's indexed primers.  
450 Sequencing was performed by the Bauer Core Facility at Harvard University. Mapping of raw  
451 fastq reads to reference PY79 genome (NC\_022898.1) was performed using Bowtie2<sup>77,78</sup>. The  
452 alignment was sorted using SAMtools<sup>79,80</sup>, data filtering and SNP variant calling was  
453 performed using the bcftools package. Mapping of raw fastq reads to phi3T genome  
454 (KY030782.1) was performed using Bowtie2 in Galaxy platform ([https://cpt.tamu.edu/galaxy-](https://cpt.tamu.edu/galaxy-pub)  
455 [pub](https://cpt.tamu.edu/galaxy-pub)) and coverage was visualized in the browser using Trackster tool. Mapping of raw SOLiD  
456 resequencing reads (168<sub>anc</sub>) to unique phi3Ts fragments was performed using CLC Genomics  
457 Workbench 11.0.1. Short phi3T fragments, to which fastq could be mapped, showed over 90%  
458 sequence identity to PY79 genome, as confirmed by BLAST. All bacterial and phage genomes  
459 sequenced during this work, were deposited at NCBI database as completed genomes and/or  
460 raw sequencing data (Table 1).

461 Raw re-sequencing data of PY79 strains<sup>50</sup> and available from B. Burton  
462 (briana.burton@wisc.edu). Raw re-sequencing data of 168 cultivated under near- zero growth  
463 conditions<sup>51</sup> are available from O. Kuipers (o.p.kuipers@rug.nl).

#### 464 **Sporulation and germination assays**

465 To examine sporulation dynamics selected strains were cultivated in MSgg medium<sup>81</sup> at 30°C,  
466 220 rpm, and total CFU and spore counts were analysed after 12, 24 and 36 hours. To access  
467 the spore count, cells were incubated at 80°C for 20min, plated on LB-agar (1.5%) and the  
468 number of obtained colonies was divided by the number of colonies obtained prior to the heat-  
469 treatment. To access the germination, the culture incubation was prolonged to 72h to allow vast  
470 majority of cells to sporulate. Next, spores were washed 2× with 0.9% NaCl, and resuspended  
471 in germination solution (0.6g KH<sub>2</sub>PO<sub>4</sub>, 1.4g K<sub>2</sub>HPO<sub>4</sub>, 0.2g (NH<sub>4</sub>)<sub>2</sub>SO<sub>4</sub>, 0.1g Na-citrate, 0.02g  
472 MgSO<sub>4</sub>×7H<sub>2</sub>O, 0.5g glucose, 3.56g L-alanine resuspended in 100ml of dH<sub>2</sub>O) to reach final  
473 OD<sub>600</sub> cca 10. Decline of OD<sub>600</sub> was measured immediately, indicating germination<sup>82</sup>.  
474 Additional assessment of germination dynamics was performed using real-time brightfield  
475 microscopy by inducing spores with L-alanine on agarose pads, as described previously<sup>57</sup>.  
476 Agarose pads (1.5%, 9 mm diameter, 1 mm height) were inoculated with 2.6 µl spore solution  
477 (3.75\*10<sup>5</sup> spores µl<sup>-1</sup>) and placed upside down into a 24-well glass-bottom microtiter plate.  
478 Germination was induced by adding 5 µl of a 200 mM L-alanine solution to the top of the pad.  
479 Germination events were monitored by changes in grey level spore intensity. The fraction of  
480 germinated spores at time t was calculated as the number of germinated spores divided by the  
481 number of dormant spores before induction (i.e.by excluding pre-germinated spores).

482

483

484

## 485 **Spore selection experiment with NCBI 3610**

486 Strains were cultivated in 10ml of MSgg medium in 100ml-glass bottles in 30°C with shaking  
487 at 220 rpm. Every 48 hours, three alternative transfer methods were applied: direct transfer of  
488 untreated cells to fresh medium, transfer of heat-treated cells (80°C for 20 min) and transfer of  
489 chemically treated cells (5% NaOH for 2 min, followed by washing in PBS). In each case, fresh  
490 cultures were initiated with 1% inoculum. Culture supernatants and cell pellets were collected  
491 prior each transfer to monitor phage release and genetic rearrangements, respectively. At each  
492 transfer, frozen stocks were preserved, to allow the analysis of subsequent steps of phage  
493 recombination in the future.

## 494 **Isolation of phage particles and phage DNA**

495 All lysogenic strains that were used as source of phages, were producing phage particles  
496 spontaneously, therefore treatment with Mitomycin C was not needed to obtain phages from  
497 culture supernatants. Lysogens were cultivated in LB medium at 37°C with shaking at  
498 200 rpm for 8h. Culture supernatants were collected, adjusted to pH of 7.0, filter-sterilized  
499 and mixed at a 1:4 rate with PEG-8000 solution (PEG-8000 20%, 116 g/l NaCl). After  
500 overnight incubation at 4°C, the solutions were centrifuged for 60 min at 12000 rpm to  
501 obtain phage precipitates. The pellets were resuspended in 1% of the initial volume in SM  
502 buffer (5.8 g/l NaCl, 0.96 g/l MgSO<sub>4</sub>, 6 g/l Tris-HCl, pH 7.5) to obtain concentrated solution  
503 of phage particles. Such phage solutions were visualized by transmission electron  
504 microscopy and used as a source of different phage variants, purified from single plaques.  
505 In plaque assay and further phage propagation from single plaques, Δ6 strain<sup>83</sup> was used as  
506 a host. Specifically, phage solutions were diluted in order to obtain well-separated single  
507 plaques. Selected plaques (differing with morphology) were carefully removed from the soft  
508 agar using sterile scalpel, resuspended in 200μl of SM buffer and used to infect

509 exponentially growing phage-free host to allow propagation of selected phage variants.  
510 Phages were subsequently propagated in soft agar and liquid host suspension until the titer  
511 reached at least  $10^9$  pfu/ml and then subjected to DNA isolation. Phage DNA was extracted  
512 using phenol-chloroform method, as described previously<sup>84</sup>.

### 513 **Transmission electron microscopy**

514 Before use, 400 mesh nickel grids with a 3-4 nm thick carbon film, CF400-Ni-UL EMS  
515 Diasum, were hydrophilized by 30 sec of electric glow discharging. Next, 5 $\mu$ l of purified  
516 phage solutions were applied onto the grids and allowed to adsorb for 1 minute. The grids  
517 were rinsed 3 times on droplets of milliQ water and subjected to staining with 2% uranyl  
518 acetate. Specifically, with a help of EM grid-grade tweezers, the grids were placed  
519 sequentially on droplets of 2% uranyl acetate solution for 10 sec, 2 sec and 20 sec. Excess  
520 uranyl acetate was wicked away using filter paper and the grids were allowed to dry  
521 overnight and stored in a desiccator until analysis. Transmission electron microscopy was  
522 performed utilizing a FEI Tecnai T12 Biotwin TEM operating at 120 kV located at the Center  
523 for Electron Nanoscopy at the Technical University of Denmark, and images were acquired  
524 using a Bottom mounted CCD, Gatan Orius SC1000WC.

### 525 **Prophage database construction and phage comparisons**

526 *Bacillus* prophage database was constructed by finding genomic coordinates using Phaster  
527 software<sup>85,86</sup> from fully assembled *Bacillus* genomes available at NCBI, followed by extraction  
528 of phage genomes using samtools package. In total, the initial database contained 350 strains,  
529 which altogether carried 1365 prophage elements. Out of these prophages, 54 were selected for  
530 further analysis according to following criteria: all prophages larger than 80kB (regardless of  
531 integration side) and all prophages that are at least 50 kB, integrated between 1.9-2.3 Mb in the  
532 chromosome, just like SP $\beta$  and phi3Ts-SP $\beta$  hybrids identified in the evolved strains.  
533 Additional prophages, categorized as SP $\beta$ -like, were retrieved the genomes that gave BLAST

534 hits to phi3T and SP $\beta$ , if these hits belonged to a prophage region that was at least 40kB  
535 (confirmed by Phaster). All genomes that were re-sequenced copies of *Bacillus subtilis* 168  
536 were removed. In addition, genomes that were starting and finishing with a prophage (likely  
537 due to misassembly), were removed (NZ\_CP032855.1). Overall, 78 *Bacillus* strains lysogenic  
538 for putative SP $\beta$ -like prophages were subjected to further analysis.

539            Interruption of *spsM* and *kamA* in all the selected lysogens was examined by  
540 genome BLAST against the sequence of an intact copy of these gene. All strains that carried a  
541 split copy of *spsM* and *kamA*, also carried a large prophage between left and right arms of these  
542 genes. In such cases, the Phaster-predicted terminal positions of the prophage was corrected to  
543 exactly match the sequence splitting *spsM* or *kamA*. Such correction was based on  
544 experimentally confirmed sequences of phage DNA. Integration genes of remaining large  
545 prophages were determined by extracting and clustering 1000bp-long prophage flanking  
546 regions using vsearch at 46% identity. These regions were then compared to well-annotated *B.*  
547 *subtilis* 168, using blastx, to find functional homologs.

548            The alignment of prophage sequences was performed in MAFFT program<sup>87</sup>,  
549 phylogenetic tree was build using FastTree<sup>88,89</sup> and visualized in CLC Main Workbench.  
550 Phylogenetic tree of *B. subtilis* host strains was constructed using open software autoMLST  
551 (<https://automlst.ziemertlab.com/>)<sup>90</sup> based on 100 shared proteins. Two strains that were not  
552 lysogenic for SP $\beta$ -like prophage (MB9\_B4 and MB9\_B6) were included in the analysis to  
553 exclude SP $\beta$  prophage from the shared pool of proteins in the tree building. The three was  
554 visualized in CLC Main Workbench. Prophage annotation was performed using RAST online  
555 annotation platform.

556

557

558 **Statistical analysis**

559 Statistical differences between two experimental groups were identified using two-tailed  
560 Student's *t*-tests assuming equal variance. No statistical methods were used to predetermine  
561 sample size and the experiments were not randomized.

562 **Authors contributions:**

563 AD, PB, ZH, CK performed experiments. AD and MLS performed bioinformatics analysis. PK  
564 performed electron microscopy, GM performed genome sequencing and analyzed the data, BB  
565 and BMB shared sequencing data. AD and ATK designed the study. AD wrote the manuscript.  
566 All authors contributed to final version of the manuscript.

567

568 **Acknowledgements:**

569 The authors thank M. Kilstrup, P. Sazinas, K. Middleboe, D. Castillio and P. Stefanic for their  
570 valuable comments. We are profoundly grateful to O. Kuipers, A. de Jong and W. Overkamp  
571 from University of Groningen, for sharing their raw sequencing data and all relevant  
572 information, which allowed us to finalize the manuscript. This project has received funding  
573 from the European Union's Horizon 2020 research and innovation programme under the Marie  
574 Skłodowska-Curie grant agreement No 713683 (H.C. Ørsted COFUND to A.D.), Individual  
575 grant from Friedrich Schiller University Jena to support postdoc researchers to A.D., and  
576 supported by the Danish National Research Foundation (DNRF137) for the Center for  
577 Microbial Secondary Metabolites. Funded in part by NIH R01GM121865 to BMB.

578

579

580



581 **Figure legends:**

582 **Figure 1.** Changes within *B. subtilis* prophage sequence and integration site observed after  
583 prolonged sporulation selection regime. A) Experimental evolution with sporulation selection  
584 regime leads to spontaneous release of phage particles by the evolved strains<sup>44</sup>. B). Overnight  
585 culture of evolved *B. subtilis* strain B410mB (*amyE::mKate*, shown in red) was diluted 100×  
586 and spotted on the lawn of undiluted *B. subtilis* ancestor strain (*amyE::gfp*, shown in green),  
587 resulting in a clearance zone, and growth of B410mB in that zone. The same experiment was  
588 performed using 100x diluted culture of ancestor strain (*amyE::mKate*) on a lawn of undiluted  
589 ancestor (*amyE::gfp*), as control. Scale bar=2.5mm. C) Schematic representation of genome  
590 rearrangements in one of the phage-releasing evolved strains (B310mA), compared to the  
591 ancestor (Anc). The evolved strains carry a hybrid prophage phi3Ts-SPβ. Fragments of phi3Ts  
592 are shown in black, while fragments of SPβ are shown in pink. Below, schematic representation  
593 of phage genomes, spontaneously released by B310mA. D) Schematic comparison of phi3Ts  
594 genome, with genome of Bacillus phage phi3T (KY030782.1). Fragment ‘s’ which is unique  
595 for phi3Ts, can be detected within prophage genomes of 6 *B. subtilis* strains, isolated in  
596 different parts of the world, specifically: SRCM103612 (South Korea), MB9\_B1 and MB8\_B1  
597 (Denmark), JAAA (China), HMNig-2 (Egypt) and SSJ-1 (South Korea).

598 **Figure 2.** Extrachromosomal fragments of phage DNA, detected in the evolved strains. Top:  
599 Genome comparison of phi3Ts and SPβ (Query cover=58%, Percent Identity=99.73%), where  
600 regions of high homology (73.6-100%) are shown in grey, and regions of 99% homology are  
601 connected. Segments that are unique for phi3Ts, or SPβ are highlighted in black and pink,  
602 respectively. Phage genomes are arranged according to their integration into the host  
603 chromosome, which is represented in red. Below: extrachromosomal phage DNA fragments  
604 detected during PacBio sequencing, colored according to their homology to phi3Ts, SPβ, or  
605 fragments of host chromosome flanking phage integration sites. Fragments are ordered

606 according to sequencing coverage relative to the chromosomal region, which is represented as  
607 bar chart on the left.

608 **Figure 3.** Detection of phi3Ts DNA in the ancestor strain *B. subtilis* 168 through mapping of  
609 raw sequencing reads. Top: Representation of phi3Ts genome according to its homology to  
610 SPβ prophage. Fragments of high homology to SPβ (73.6-100%) are shown in grey, while  
611 fragments that are unique to phi3Ts are shown in black. Bars 1,2 and 3 correspond to DNA  
612 sequences that are unique for phi3Ts and that were used as targets for raw reads mapping (lower  
613 part). Green and red bars represent reads obtained from forward and reverse strands,  
614 respectively.

615 **Figure 4.** Effect of phi3T infection on *B. subtilis* sporulation and germination dynamics. A)  
616 Sporulation dynamics. Percentage of spores compared to total cell count, were examined in *B.*  
617 *subtilis* 3610 and the same strain infected with phi3T phage, in 3 different time points of growth  
618 in minimal medium (MSgg). Data represent an average from 4 biological replicates, error bars  
619 correspond to standard error.

620 **Figure 5.** Overview of prophage elements of natural *Bacillus* sp. isolates. A) Prophage  
621 elements were extracted from fully assembled genomes of *Bacillus* sp. and plotted according  
622 to size and integration position in the chromosome. Cluster of large prophages, integrated in  
623 the area of replication terminus could be detected (black dotted line). B) Schematic  
624 representation of SPβ-like prophage found in *B. subtilis* SRCM 103612, isolated from  
625 traditional Korean food. The prophage genome was colored according to its homology to  
626 phi3Ts and SPβ. Extrachromosomal phage DNA found in this strain is matching left and right  
627 arms of the chromosomal prophage.

628 **Figure 6.** Natural diversity of SPβ-like phages. A). Phylogenetic tree of *B. subtilis* strains that  
629 carry SPβ-like prophage in *spsM* or *kamA* gene, and two control strains that are free from such

630 prophage. The tree was arbitrarily divided into 6 clades. B) Phylogenetic tree of SP $\beta$ -like  
 631 prophages hosted by the strains in A). Inner circle shows prophage integration site, while outer  
 632 circle indicates presence/absence of conjugative element ICEBs1, which blocks SP $\beta$  lytic cycle  
 633 C). Selected prophages of *Bacillus* sp. colored according to their homology to phi3T and SP $\beta$ .  
 634 The upper 4 sequences integrate either in *kamA* or *spsM* and clearly belong to SP $\beta$ -like phages.  
 635 Bottom four sequences come from other *Bacillus* species, and although they are more distant  
 636 to phi3T or SP $\beta$ , they still carry segments of high homology with these phages. Explanation of  
 637 ICEBs1 figure legend: intact – intact copy (100% identity to *B. subtilis* 168 or NCBI 3610) of  
 638 ICEBs1 conjugative element is present; negative – lack of BLAST hits to ICEBs1 sequence;  
 639 partial – at least 70% of ICEBs1 sequence is present; residual – less than 5% of ICEBs1  
 640 sequence is present.

641 **Table 1** | List of bacterial strain and phages subjected to genome sequencing with  
 642 corresponding NCBI accession numbers.

Name of bacterial strain/phage	Data	Accession number
B310mA	Complete genome	CP051860
B410mB	Complete genome	CP053102*
B410wtB	Complete genome	CP052842*
B310mA	Sequencing reads (Illumina)	SRR11561554
B410mB	Sequencing reads (Illumina)	SRR1156151
B410wtB	Sequencing reads (Illumina)	SRR11561552
168 <sub>ancestor</sub>	Sequencing reads (SOLiD)	SRR11559011
NCBI 3610	Sequencing reads (Illumina)	SRR11559035
15.1	Sequencing reads (Illumina)	SRR11566357
16.1	Sequencing reads (Illumina)	SRR11566355

16.2	Sequencing reads (Illumina)	SRR11566354
phi3Ts	Complete genome	MT366945
Hyb1 <sup>phi3Ts-SPβ</sup>	Complete genome	MT366946
Hyb2 <sup>phi3Ts-SPβ</sup>	Complete genome	MT366947
Hyb3 <sup>phi3Ts-SPβ</sup>	Complete genome	MT366948
phi3Ts	Sequencing reads (Illumina)	SRR11587866
Hyb1 <sup>phi3Ts-SPβ</sup>	Sequencing reads (Illumina)	SRR11587864
Hyb2 <sup>phi3Ts-SPβ</sup>	Sequencing reads (Illumina)	SRR11587865
Hyb3 <sup>phi3Ts-SPβ</sup>	Sequencing reads (Illumina)	SRR11587867

643 \*extrachromosomal phage fragments: B410wtB - CP052843; B410mB – supplementary  
 644 dataset 4.

645

- 646 1. Knowles, B. *et al.* Lytic to temperate switching of viral communities. *Nature* **531**,  
 647 466–470 (2016).
- 648 2. Koskella, B. & Brockhurst, M. A. Bacteria–phage coevolution as a driver of ecological  
 649 and evolutionary processes in microbial communities. *FEMS Microbiol. Rev.* **38**, 916–  
 650 931 (2014).
- 651 3. Azam, A. H. & Tanji, Y. Bacteriophage-host arm race: an update on the mechanism of  
 652 phage resistance in bacteria and revenge of the phage with the perspective for phage  
 653 therapy. *Appl. Microbiol. Biotechnol.* **103**, 2121–2131 (2019).
- 654 4. Howard-Varona, C., Hargreaves, K. R., Abedon, S. T. & Sullivan, M. B. Lysogeny in  
 655 nature: mechanisms, impact and ecology of temperate phages. *ISME J.* **11**, 1511–1520  
 656 (2017).

- 657 5. Harrison, E. & Brockhurst, M. A. Ecological and evolutionary benefits of temperate  
658 phage: what does or doesn't kill you makes you stronger. *BioEssays* **39**, 1700112  
659 (2017).
- 660 6. Davies, E. V., Winstanley, C., Fothergill, J. L. & James, C. E. The role of temperate  
661 bacteriophages in bacterial infection. *FEMS Microbiol. Lett.* **363**, fnw015 (2016).
- 662 7. Kim, M. S. & Bae, J. W. Lysogeny is prevalent and widely distributed in the murine  
663 gut microbiota. *ISME J.* **12**, 1127–1141 (2018).
- 664 8. Štefanič, P., Kraigher, B., Lyons, N. A., Kolter, R. & Mandić-Mulec, I. Kin  
665 discrimination between sympatric *Bacillus subtilis* isolates. *Proc. Natl. Acad. Sci.*  
666 *U.S.A.* **112**, 14042–14047 (2015).
- 667 9. Lyons, N. A., Kraigher, B., Štefanič, P., Mandić-Mulec, I. & Kolter, R. A  
668 combinatorial kin discrimination system in *Bacillus subtilis*. *Curr. Biol.* **26**, 733–742  
669 (2016).
- 670 10. Canchaya, C., Proux, C., Fournous, G., Bruttin, A. & Brüßow, H. Prophage genomics.  
671 *Microbiol. Mol. Biol. Rev.* **67**, 238–76, (2003).
- 672 11. Bérard, S. *et al.* Aligning the unalignable: bacteriophage whole genome alignments.  
673 *BMC Bioinformatics* **17**, 30 (2016).
- 674 12. Botstein, D. A theory of modular evolution for bacteriophages. *Ann. N. Y. Acad. Sci.*  
675 **354**, 484–491 (1980).
- 676 13. Hatfull, G. F. & Hendrix, R. W. Bacteriophages and their genomes. *Curr. Opin. Virol.*  
677 **1**, 298–303 (2011).
- 678 14. De Paepe, M. *et al.* Temperate phages acquire DNA from defective prophages by  
679 relaxed homologous recombination: the role of Rad52-like recombinases. *PLoS Genet.*

- 680           **10**, (2014).
- 681   15.   Swenson, K. M., Guertin, P., Deschênes, H. & Bergeron, A. Reconstructing the  
682       modular recombination history of *Staphylococcus aureus* phages. *BMC Bioinformatics*  
683       **14**, S17 (2013).
- 684   16.   Morris, P., Marinelli, L. J., Jacobs-Sera, D., Hendrix, R. W. & Hatfull, G. F. Genomic  
685       characterization of mycobacteriophage giles: Evidence for phage acquisition of host  
686       DNA by illegitimate recombination. *J. Bacteriol.* **190**, 2172–2182 (2008).
- 687   17.   Bobay, L.-M., Touchon, M. & Rocha, E. P. C. Manipulating or superseding host  
688       recombination functions: A dilemma that shapes phage evolvability. *PLoS Genet.* **9**,  
689       e1003825 (2013).
- 690   18.   Spancake, G. A., Hemphill, H. E. & Fink, P. S. Genome organization of Sp beta c2  
691       bacteriophage carrying the *thyP3* gene. *J. Bacteriol.* **157**, 428–34 (1984).
- 692   19.   Fillol-Salom, A. *et al.* Bacteriophages benefit from generalized transduction. *PLOS*  
693       *Pathog.* **15**, e1007888 (2019).
- 694   20.   Uchiyama, J. *et al.* Intragenus generalized transduction in *Staphylococcus* spp. by a  
695       novel giant phage. *ISME J.* **8**, 1949–1952 (2014).
- 696   21.   Morse, M. L., Lederberg, E. M. & Lederberg, J. Transduction in *Escherichia coli* K-  
697       12. *Genetics* **41**, 142–56 (1956).
- 698   22.   Fukumaki, Y., Shimada, K. & Takagi, Y. Specialized transduction of Colicin E1 DNA  
699       in *Escherichia coli* K-12 by phage Lambda. *Proc. Natl. Acad. Sci. U. S. A.* **73**, 3238–  
700       3242
- 701   23.   Penadés, J. R., Chen, J., Quiles-Puchalt, N., Carpena, N. & Novick, R. P.  
702       Bacteriophage-mediated spread of bacterial virulence genes. *Current Opinion in*

- 703            *Microbiology* **23**, 171–178 (2015).
- 704    24.    Kupczok, A. *et al.* Rates of mutation and recombination in *Siphoviridae* phage genome  
705            evolution over three decades. *Mol. Biol. Evol.* **35**, 1147–1159 (2018).
- 706    25.    Yahara, K., Lehours, P. & Vale, F. F. Analysis of genetic recombination and the pan-  
707            genome of a highly recombinogenic bacteriophage species. *Microb. genomics* **5**,  
708            (2019).
- 709    26.    Yamamoto, N., Wohlhieter, J. A., Gemski, P. & Baron, L. S.  $\lambda$ immP22dis: A hybrid of  
710            coliphage  $\lambda$  with both immunity regions of Salmonella phage P22. *Mol. Gen. Genet.*  
711            *MGG* **166**, 233–243
- 712    27.    Botstein, D. & Herskowitz, I. Properties of hybrids between Salmonella phage P22 and  
713            coliphage  $\lambda$ . *Nature* **251**, 584–589 (1974).
- 714    28.    Feiner, R. *et al.* A new perspective on lysogeny: prophages as active regulatory  
715            switches of bacteria. *Nat. Rev. Microbiol.* **13**, 641–650 (2015).
- 716    29.    Abe, K. *et al.* Developmentally-regulated excision of the SP $\beta$  prophage reconstitutes a  
717            gene required for spore envelope maturation in *Bacillus subtilis*. *PLoS Genet.* **10**,  
718            e1004636 (2014).
- 719    30.    Abe, K., Takamatsu, T. & Sato, T. Mechanism of bacterial gene rearrangement: SprA-  
720            catalyzed precise DNA recombination and its directionality control by SprB ensure the  
721            gene rearrangement and stable expression of *spsM* during sporulation in *Bacillus*  
722            *subtilis*. *Nucleic Acids Res.* **45**, 6669–6683 (2017).
- 723    31.    Haraldsen, J. D. & Sonenshein, A. L. Efficient sporulation in *Clostridium difficile*  
724            requires disruption of the  $\sigma$ K gene. *Mol. Microbiol.* **48**, 811–821 (2003).
- 725    32.    Stragier, P., Kunkel, B., Kroos, L. & Losick, R. Chromosomal rearrangement

- 726 generating a composite gene for a developmental transcription factor. *Science* **243**,  
727 507–512 (1989).
- 728 33. Wood, J. P. *et al.* Environmental persistence of *Bacillus anthracis* and *Bacillus subtilis*  
729 spores. *PLoS One* **10**, e0138083 (2015).
- 730 34. Cano, R. J. & Borucki, M. K. Revival and identification of bacterial spores in 25- to  
731 40-million-year-old Dominican amber. *Science* **268**, 1060–1064 (1995).
- 732 35. Sanchez-Vizueté, P. *et al.* Identification of *ypqP* as a new *Bacillus subtilis* biofilm  
733 determinant that mediates the protection of *Staphylococcus aureus* against  
734 antimicrobial agents in mixed-species communities. *Appl. Environ. Microbiol.* **81**,  
735 109–118 (2015).
- 736 36. Kimura, T., Amaya, Y., Kobayashi, K., Ogasawara, N. & Sato, T. Repression of *sigK*  
737 intervening (*skin*) element gene expression by the CI-like protein SknR and effect of  
738 SknR depletion on growth of *Bacillus subtilis* cells. *J. Bacteriol.* **192**, 6209–6216  
739 (2010).
- 740 37. Kunkel, B., Losick, R. & Stragier, P. The *Bacillus subtilis* gene for the developmental  
741 transcription factor  $\sigma(K)$  is generated by excision of a dispensable DNA element  
742 containing a sporulation recombinase gene. *Genes Dev.* **4**, 525–535 (1990).
- 743 38. Pyne, M. E., Liu, X., Moo-Young, M., Chung, D. A. & Chou, C. P. Genome-directed  
744 analysis of prophage excision, host defence systems, and central fermentative  
745 metabolism in *Clostridium pasteurianum*. *Sci. Rep.* **6**, 26228 (2016).
- 746 39. Sohail, A., Hayes, C. S., Divvela, P., Setlow, P. & Bhagwat, A. S. Protection of DNA  
747 by  $\alpha/\beta$ -type small, acid-soluble proteins from *Bacillus subtilis* spores against cytosine  
748 deamination. *Biochemistry* **41**, 11325–11330 (2002).



- 749 40. Ki, S. L., Bumbaca, D., Kosman, J., Setlow, P. & Jedrzejewski, M. J. Structure of a  
750 protein-DNA complex essential for DNA protection in spores of *Bacillus* species.  
751 *Proc. Natl. Acad. Sci. U. S. A.* **105**, 2806–2811 (2008).
- 752 41. Jiang, M., Grau, R. & Perego, M. Differential processing of propeptide inhibitors of  
753 rap phosphatases in *Bacillus subtilis*. *J. Bacteriol.* **182**, 303–310 (2000).
- 754 42. Serra, C. R., Earl, A. M., Barbosa, T. M., Kolter, R. & Henriques, A. O. Sporulation  
755 during growth in a gut isolate of *Bacillus subtilis*. *J. Bacteriol.* **196**, 4184–4196 (2014).
- 756 43. Silver-Mysliwiec, T. H. & Bramucci, M. G. Bacteriophage-enhanced sporulation:  
757 Comparison of spore-converting bacteriophages PMB12 and SP10. *J. Bacteriol.* **172**,  
758 1948–1953 (1990).
- 759 44. Martin, M. *et al.* De novo evolved interference competition promotes the spread of  
760 biofilm defectors. *Nat. Commun.* **8**, 15127 (2017).
- 761 45. Eleina England, by M. & Bell Professor of Biology, S. P. Effects of cell growth and a  
762 mobile genetic element on propagation of the phages SP16 and SP-beta in *Bacillus*  
763 *subtilis* (2014).
- 764 46. Warner, F. D. *et al.* Characterization of SPP: a temperate bacteriophage from *Bacillus*  
765 *subtilis* 168M. *Can J Microbiol* **23**, 45-51 (1976).
- 766 47. Erez, Z. *et al.* Communication between viruses guides lysis-lysogeny decisions. *Nature*  
767 **541**, 488–493 (2017).
- 768 48. Dennehy, J. J. Bacteriophage Ecology: Population growth, evolution, and impact of  
769 bacterial viruses. Part of Advances in Molecular and Cellular Biology - *The Quarterly*  
770 *Review of Biology* (2010).
- 771 49. Gallegos-Monterrosa, R., Mhatre, E. & Kovács, A. T. Specific *Bacillus subtilis* 168

- 772 variants form biofilms on nutrient- rich medium. *Microbiology* 2016;162:1922–32.ch  
773 medium. *Microbiology* **162**, 1922–1932 (2016).
- 774 50. Bose, B., Reed, S. E., Besprozvannaya, M. & Burton, B. M. Missense mutations allow  
775 a sequence-blind mutant of SpoIIIE to successfully translocate chromosomes during  
776 sporulation. *PLoS One* **11**, e0148365 (2016).
- 777 51. Overkamp, W. *et al.* Physiological and cell morphology adaptation of *Bacillus subtilis*  
778 at near-zero specific growth rates: A transcriptome analysis. *Environ. Microbiol.* **17**,  
779 346–363 (2015).
- 780 52. Omer Bendori, S., Pollak, S., Hizi, D. & Eldar, A. The RapP-PhrP quorum-sensing  
781 system of *Bacillus subtilis* strain NCIB3610 affects biofilm formation through multiple  
782 targets, due to an atypical signal-insensitive allele of RapP. *J. Bacteriol.* **197**, 592–602  
783 (2015).
- 784 53. Singh, P. K. *et al.* Mobility of the native *Bacillus subtilis* conjugative plasmid pLS20  
785 is regulated by intercellular signaling. *PLoS Genet.* **9**, e1003892 (2013).
- 786 54. Auchtung, J. M., Lee, C. A., Monson, R. E., Lehman, A. P. & Grossman, A. D.  
787 Regulation of a *Bacillus subtilis* mobile genetic element by intercellular signaling and  
788 the global DNA damage response. *Proc. Natl. Acad. Sci. U. S. A.* **102**, 12554–12559  
789 (2005).
- 790 55. Perego, M. & Hoch, J. A. Cell-cell communication regulates the effects of protein  
791 aspartate phosphatases on the phosphorelay controlling development in *Bacillus*  
792 *subtilis*. *Proc. Natl. Acad. Sci. U. S. A.* **93**, 1549–53 (1996).
- 793 56. Tovar-Rojo, F. & Setlow, P. Effects of mutant small, acid-soluble spore proteins from  
794 *Bacillus subtilis* on DNA in vivo and in vitro. *J. Bacteriol.* **173**, 4827–4835 (1991).

- 795 57. Mutlu, A. *et al.* Phenotypic memory in *Bacillus subtilis* links dormancy entry and exit  
796 by a spore quantity-quality tradeoff. *Nat. Commun.* **9**, (2018).
- 797 58. Kiesevalter, H. T. *et al.* Complete genome sequences of 13 *Bacillus subtilis* soil  
798 isolates for studying secondary metabolite diversity. *Microbiol. Resour. Announc.* **9**,  
799 (2020).
- 800 59. Bobay, L.-M., Touchon, M. & Rocha, E. P. C. Pervasive domestication of defective  
801 prophages by bacteria. *Proc. Natl. Acad. Sci.* **111**, 12127–12132 (2014).
- 802 60. Song, S., Guo, Y., Kim, J.-S., Wang, X. & Wood, T. K. Phages mediate bacterial self-  
803 recognition. *Cell Rep.* **27**, 737-749.e4 (2019).
- 804 61. Downs, D. M. & Roth, J. R. A novel P22 prophage in *Salmonella typhimurium*.  
805 *Genetics* **117**, 367–80 (1987).
- 806 62. Moreno, F. On the trapping of phage genomes in spores of *Bacillus subtilis* 168  
807 reciprocal exclusion of phages  $\phi 29$  and  $\phi e$  during outgrowth of spores. *Virology* **93**,  
808 357–368 (1979).
- 809 63. Sonenshein, A. L. Trapping of unreplicated phage DNA into spores of *Bacillus subtilis*  
810 and its stabilization against damage by  $^{32}P$  decay. *Virology* **42**, 488–495 (1970).
- 811 64. Ramírez-Guadiana, F. H., Meeske, A. J., Wang, X., Rodrigues, C. D. A. & Rudner, D.  
812 Z. The *Bacillus subtilis* germinant receptor GerA triggers premature germination in  
813 response to morphological defects during sporulation. *Mol. Microbiol.* **105**, 689–704  
814 (2017).
- 815 65. Lewis, R. J., Brannigan, J. A., Offen, W. A., Smith, I. & Wilkinson, A. J. An  
816 evolutionary link between sporulation and prophage induction in the structure of a  
817 repressor:anti-repressor complex. *J. Mol. Biol.* **283**, 907–912 (1998).

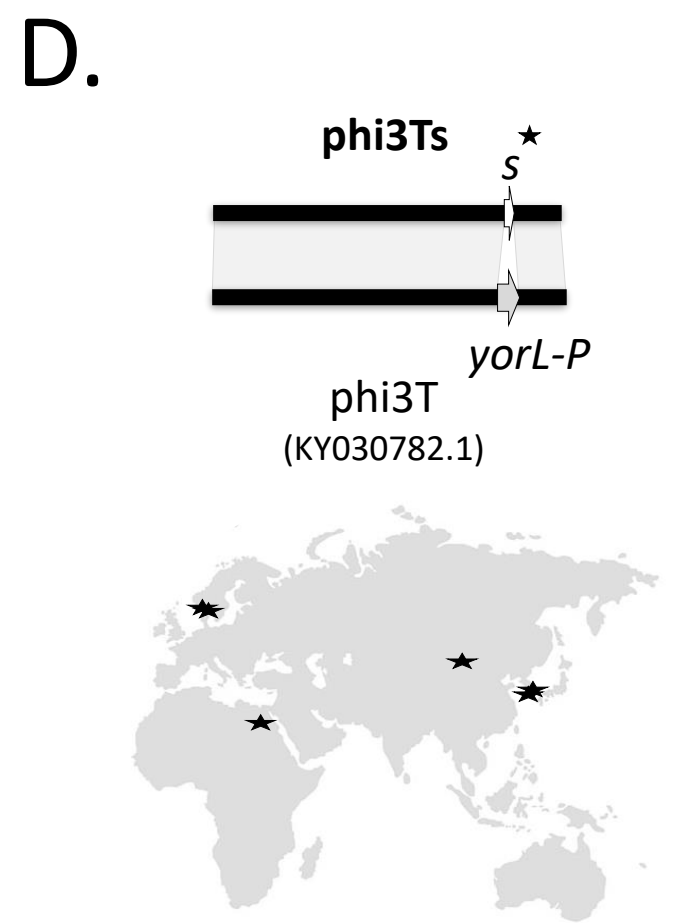
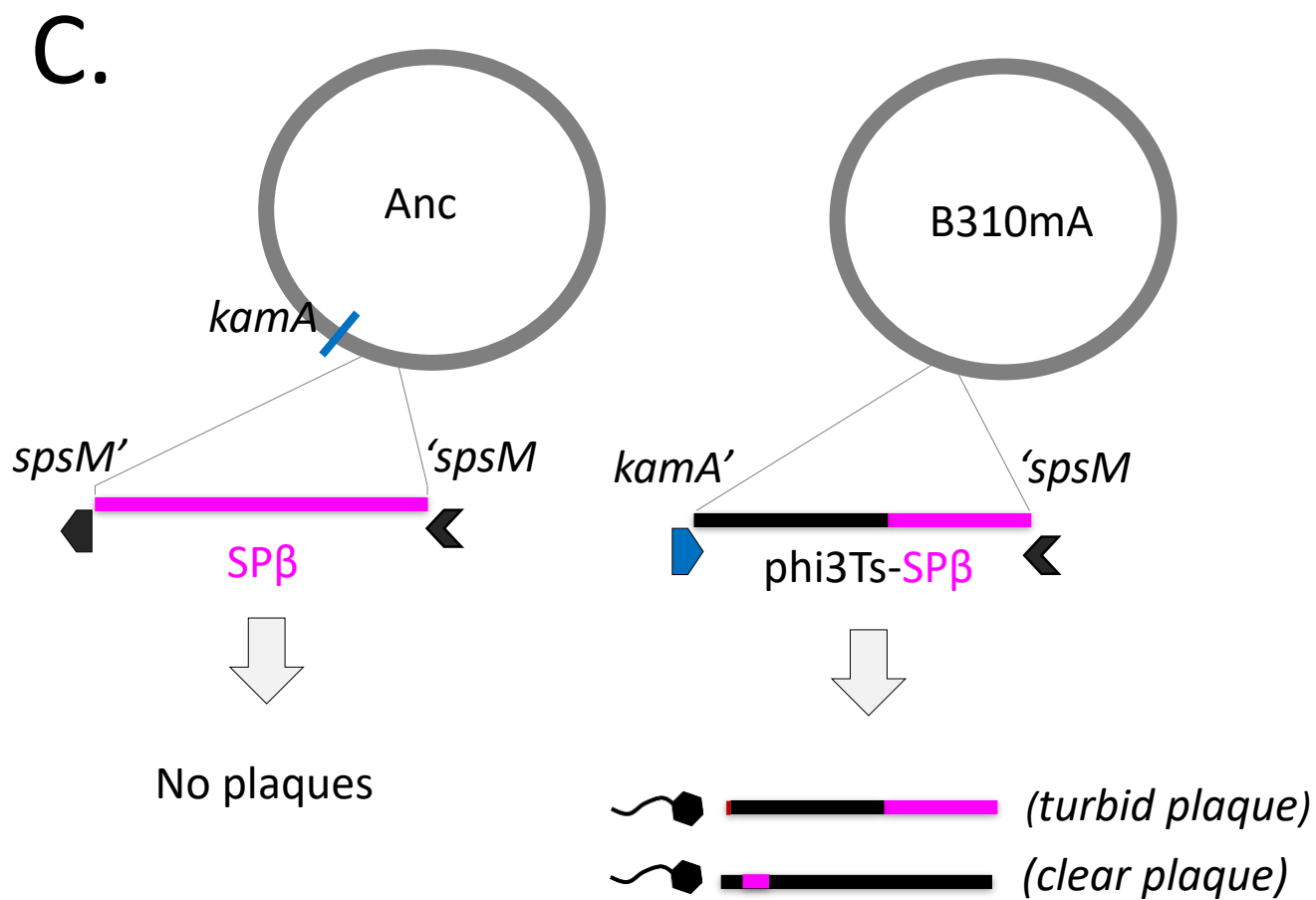
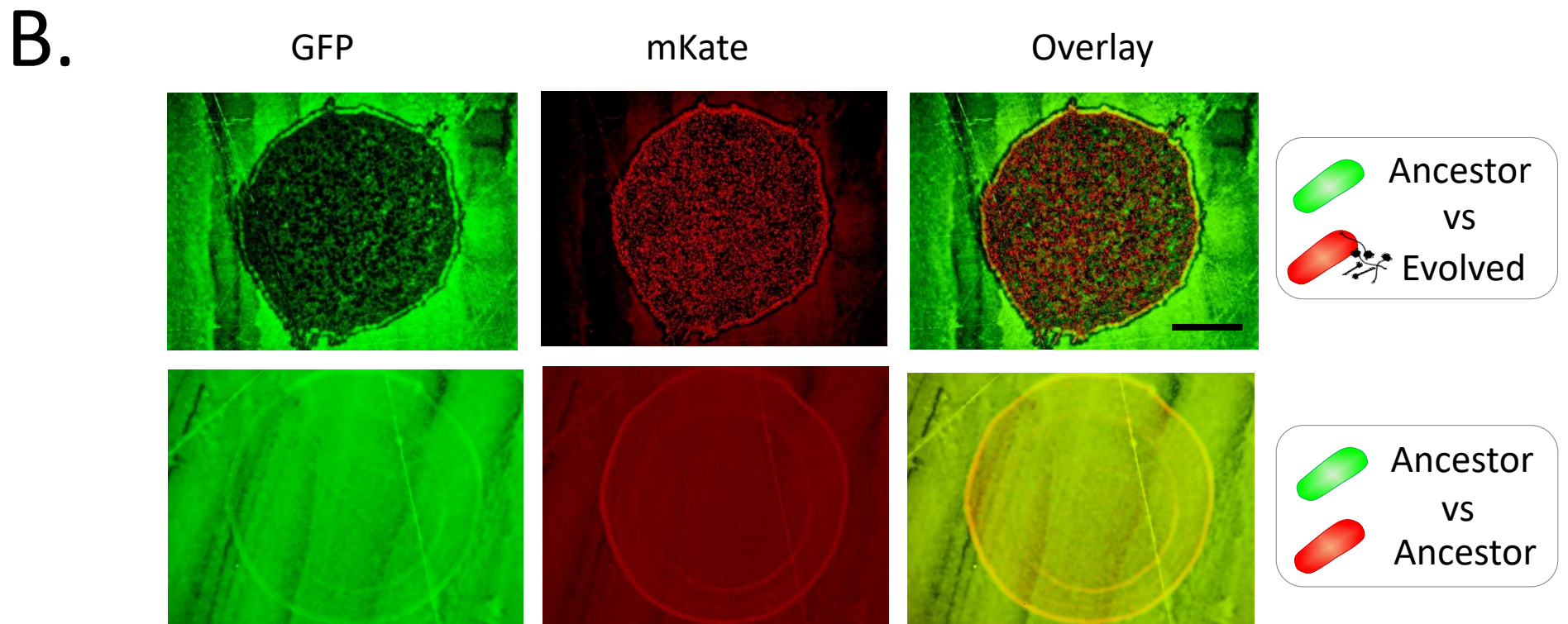
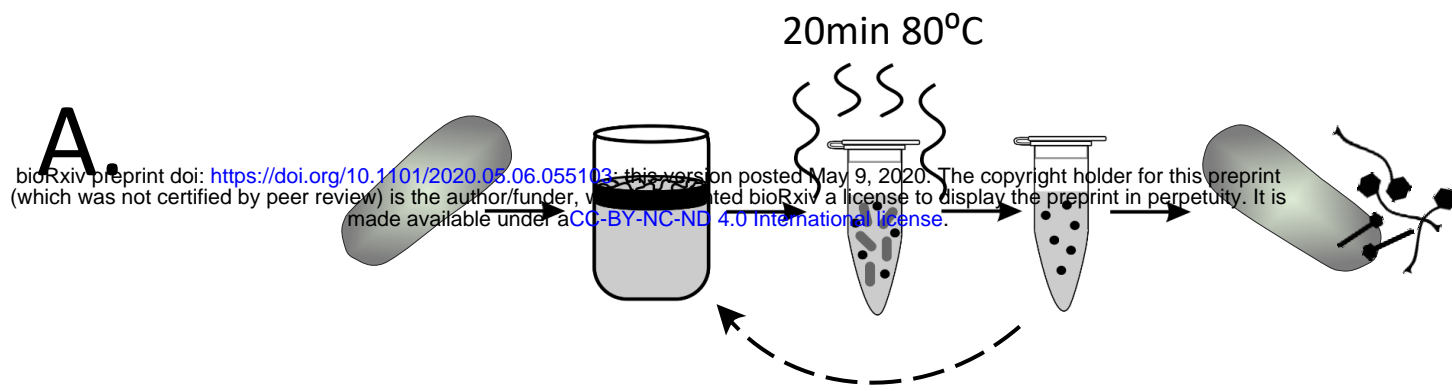
- 818 66. Sonenshein, A. L. Bacteriophages: How bacterial spores capture and protect phage  
819 DNA. *Current Biology* **16**, (2006).
- 820 67. Castilla-Llorente, V., Muñoz-Espín, D., Villar, L., Salas, M. & Meijer, W. J. J. Spo0A,  
821 the key transcriptional regulator for entrance into sporulation, is an inhibitor of DNA  
822 replication. *EMBO J.* **25**, 3890–3899 (2006).
- 823 68. Babel, H. *et al.* Ratiometric population sensing by a pump-probe signaling system in  
824 *Bacillus subtilis*. *Nat. Commun.* **11**, 1–13 (2020).
- 825 69. Paik, S. H., Chakicherla, A. & Hansen, J. N. Identification and characterization of the  
826 structural and transporter genes for, and the chemical and biological properties of,  
827 sublancin 168, a novel lantibiotic produced by *Bacillus subtilis* 168. *J. Biol. Chem.*  
828 **273**, 23134–23142 (1998).
- 829 70. Denham, E. L. *et al.* Differential expression of a prophage-encoded glycoicin and its  
830 immunity protein suggests a mutualistic strategy of a phage and its host. *Sci. Rep.* **9**,  
831 2845 (2019).
- 832 71. Lazarevic, V. *et al.* Nucleotide sequence of the *Bacillus subtilis* temperate  
833 bacteriophage SP $\beta$ c2. *Microbiology* **145**, 1055–1067 (1999).
- 834 72. Moeller, R., Setlow, P., Reitz, G. & Nicholson, W. L. Roles of small, acid-soluble  
835 spore proteins and core water content in survival of *Bacillus subtilis* spores exposed to  
836 environmental solar UV radiation. *Appl. Environ. Microbiol.* **75**, 5202–8 (2009).
- 837 73. Schultz, D., Wolynes, P. G., Jacob, E. Ben & Onuchic, J. N. Deciding fate in adverse  
838 times: Sporulation and competence in *Bacillus subtilis*.
- 839 74. de Vega, M. The minimal *Bacillus subtilis* nonhomologous end joining repair  
840 machinery. *PLoS One* **8**, e64232 (2013).

- 841 75. Lyons, N. A., Kraigher, B., Stefanic, P., Mandic-Mulec, I. & Kolter, R. A  
842 Combinatorial kin discrimination system in *Bacillus subtilis*. *Curr. Biol.* **26**, 733–42  
843 (2016).
- 844 76. Dey, A. *et al.* Sibling rivalry in *Myxococcus xanthus* is mediated by kin recognition  
845 and a polyploid prophage. *J. Bacteriol.* **198**, 994–1004 (2016).
- 846 77. Langmead, B., Wilks, C., Antonescu, V. & Charles, R. Scaling read aligners to  
847 hundreds of threads on general-purpose processors. *Bioinformatics* **35**, 421–432  
848 (2019).
- 849 78. Langmead, B. & Salzberg, S. L. Fast gapped-read alignment with Bowtie 2. *Nat.*  
850 *Methods* **9**, 357–359 (2012).
- 851 79. Li, H. *et al.* The Sequence Alignment/Map format and SAMtools. *Bioinformatics* **25**,  
852 2078–2079 (2009).
- 853 80. Li, H. A statistical framework for SNP calling, mutation discovery, association  
854 mapping and population genetical parameter estimation from sequencing data.  
855 *Bioinformatics* **27**, 2987–2993 (2011).
- 856 81. Branda, S. S., Gonzalez-Pastor, J. E., Ben-Yehuda, S., Losick, R. & Kolter, R. Fruiting  
857 body formation by *Bacillus subtilis*. *Proc. Natl. Acad. Sci. U. S. A.* **98**, 11621–11626  
858 (2001).
- 859 82. Harwood, C. R. & Cutting, S. M. Molecular biological methods for *Bacillus*. (Wiley,  
860 1990).
- 861 83. Westers, H. *et al.* Genome engineering reveals large dispensable regions in *Bacillus*  
862 *subtilis*. *Mol. Biol. Evol.* **20**, 2076–2090 (2003).
- 863 84. Tóth, I., Sváb, D., Bálint, B., Brown-Jaque, M. & Maróti, G. Comparative analysis of

- 864 the Shiga toxin converting bacteriophage first detected in *Shigella sonnei*. *Infect.*  
865 *Genet. Evol.* **37**, 150–157 (2016).
- 866 85. Zhou, Y., Liang, Y., Lynch, K. H., Dennis, J. J. & Wishart, D. S. PHAST: A Fast  
867 Phage Search Tool. *Nucleic Acids Res.* **39**, (2011).
- 868 86. Arndt, D. *et al.* PHASTER: a better, faster version of the PHAST phage search tool.  
869 *Nucleic Acids Res.* **44**, W16–W21 (2016).
- 870 87. Katoh, K. & Standley, D. M. MAFFT multiple sequence alignment software version 7:  
871 Improvements in performance and usability. *Mol. Biol. Evol.* **30**, 772–780 (2013).
- 872 88. Price, M. N., Dehal, P. S. & Arkin, A. P. FastTree: computing large minimum  
873 evolution trees with profiles instead of a distance matrix. *Mol. Biol. Evol.* **26**, 1641–  
874 1650 (2009).
- 875 89. Price, M. N., Dehal, P. S. & Arkin, A. P. FastTree 2 - Approximately maximum-  
876 likelihood trees for large alignments. *PLoS One* **5**, (2010).
- 877 90. Alanjary, M., Steinke, K. & Ziemert, N. AutoMLST: an automated web server for  
878 generating multi-locus species trees highlighting natural product potential. *Nucleic*  
879 *Acids Res.* **47**, W276–W282 (2019).
- 880 91. Konkol, M. A., Blair, K. M. & Kearns, D. B. Plasmid-encoded ComI inhibits  
881 competence in the ancestral 3610 strain of *Bacillus subtilis*. *J. Bacteriol.* **195**, 4085–  
882 4093 (2013).
- 883 92. Tucker, R. G. Acquisition of thymidylate synthetase activity by a thymine-requiring  
884 mutant of *Bacillus subtilis* following infection by the temperate phage  $\phi$ 3. *J. Gen. Virol*  
885 **4**, (1969).

886

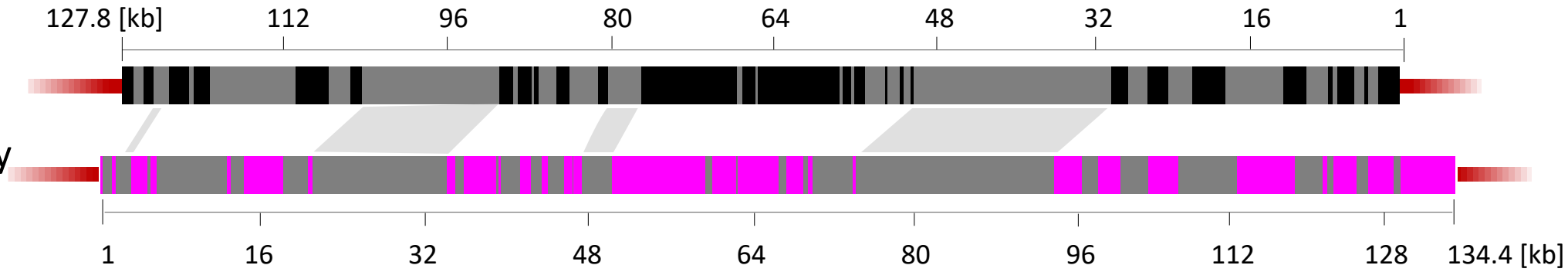




phi3Ts

Legend:

- unique for phi3Ts
- unique for SPβ
- region of high homology



SPβ

Relative coverage

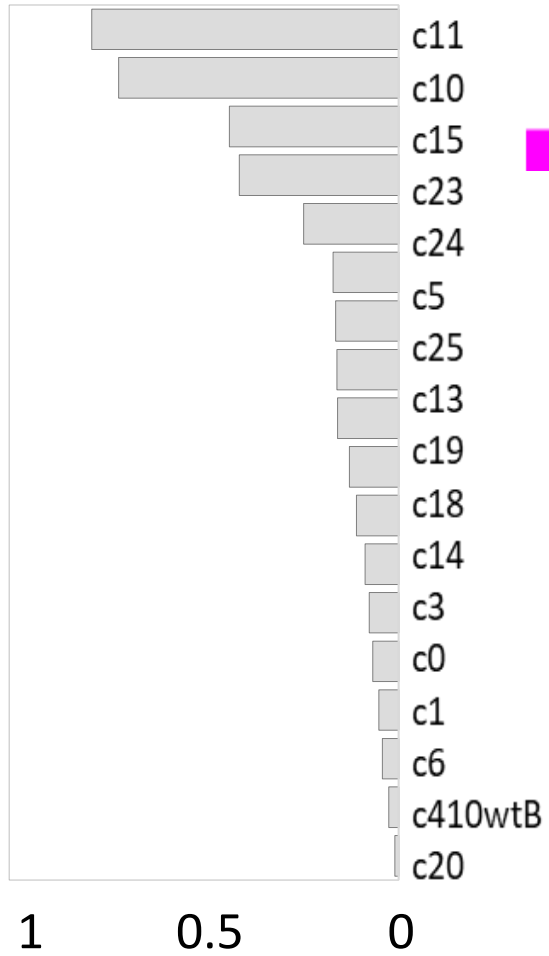




**Fig. 3**

- unique
- high homology with SPβ

# phi3Ts

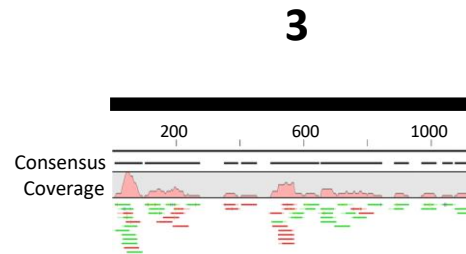
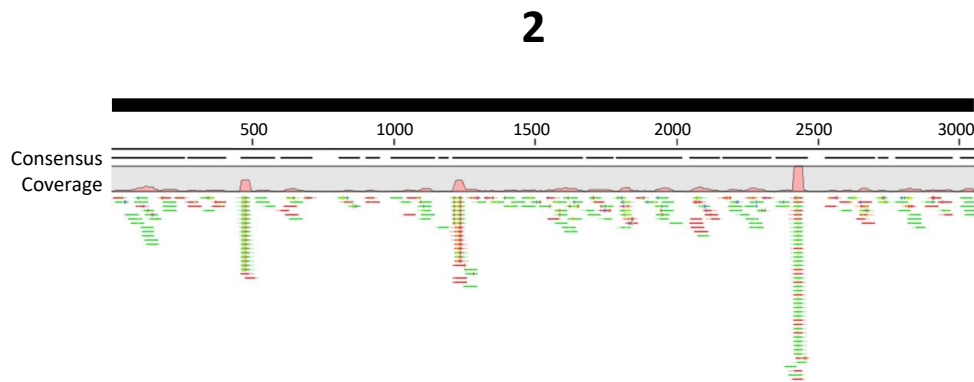
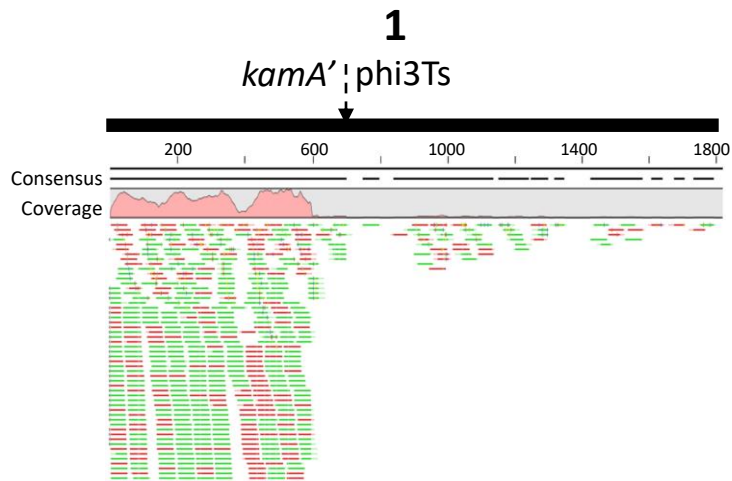
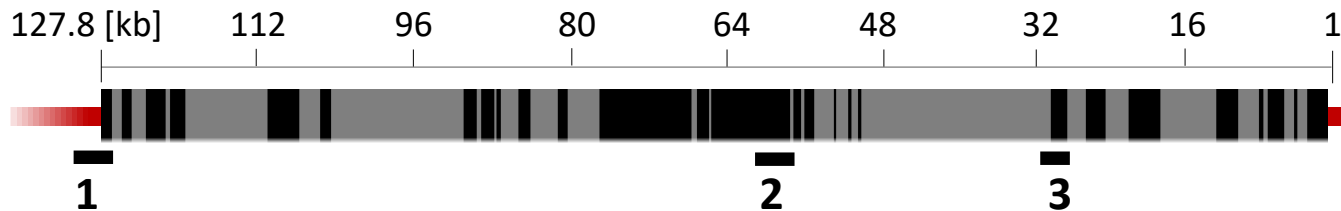


**Fig. 4**

